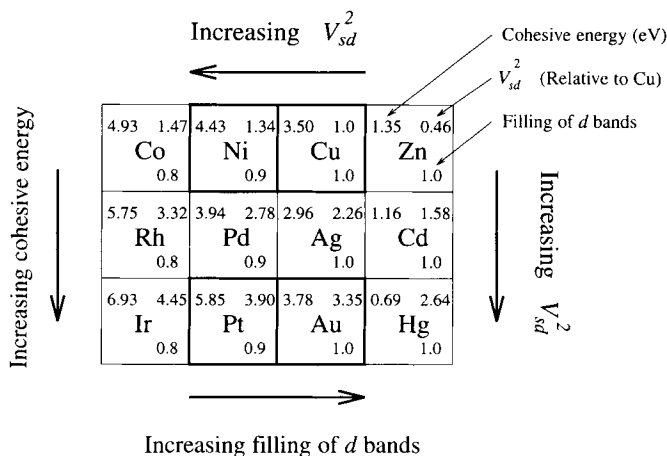


FIG. 4 The s - d coupling matrix element (V_{sd}^2 ; refs 17, 18), the filling of the metal d bands and the cohesive energy²² for metals in the vicinity of gold in the periodic table. The filling of the metal d bands is taken as a measure of the filling of the adsorbate-metal d antibonding state. The largest adsorbate-metal d repulsion, and hence the largest nobleness in terms of the surface reactivity, is obtained by maximizing V_{sd}^2 and having an antibonding state filling of one. This is obtained for gold. The nobleness in terms of ability to resist corrosion and dissolution further involves the cohesive energy of the metals. This energy is largest for the $5d$ metals like Ir and Pt and adds particularly to the nobleness of these metals.



explains why gold is able to form metallic alloys, because the bond lengths here are very long. □

Received 24 February; accepted 27 June 1995.

- Hayden, B. E. & Lamont, C. L. A. *Phys. Rev. Lett.* **63**, 1823–1825 (1989).
- Hodgson, A., Moryl, J., Traversaro, P. & Zhao, H. *Nature* **356**, 501–504 (1992).
- Michelsen, H. A., Rettner, C. T. & Auerbach, D. J. *Phys. Rev. Lett.* **69**, 2678–2681 (1992).
- Michelsen, H. A., Rettner, C. T., Auerbach, D. J. & Zare, R. N. *J. chem. Phys.* **98**, 8294–8307 (1993).
- Berger, H. F., Leisch, M., Winkler, A. & Rendulic, K. D. *Chem. Phys. Lett.* **175**, 425–428 (1990).
- Robota, H. J., Vielhaber, W., Lin, M. C., Segner, J. & Ertl, G. *Surf. Sci.* **155**, 101–120 (1985).
- Brown, J. K., Luntz, A. & Schultz, P. A. *J. chem. Phys.* **95**, 3767–3774 (1991).
- Jaffey, D. M. & Madix, R. J. *Surf. Sci.* **311**, 159–171 (1994).
- Hammer, B., Scheffler, M., Jacobsen, K. W. & Nørskov, J. K. *Phys. Rev. Lett.* **73**, 1400–1403 (1994).
- White, J. A., Bird, D. M., Payne, M. C. & Stich, I. *Phys. Rev. Lett.* **73**, 1404–1407 (1994).
- Gross, A., Hammer, B., Scheffler, M. & Brenig, W. *Phys. Rev. Lett.* **73**, 3121–3124 (1994).

- Feibelman, P. J. & Harris, J. *Nature* **372**, 135–136 (1994).
- Hammer, B. & Scheffler, M. *Phys. Rev. Lett.* **74**, 3487–3490 (1995).
- Lundqvist, B. I., Gunnarsson, O., Hjelmberg, H. & Nørskov, J. K. *Surf. Sci.* **89**, 196–225 (1979).
- Holloway, S., Lundqvist, B. I. & Nørskov, J. K. in *Proc. int. Congr. on Catalysis* 85–95 (Chemie, Berlin, 1984).
- Nørskov, J. K. *Rep. Prog. Phys.* **53**, 1253–1295 (1990).
- Andersen, O. K., Jepsen, O. & Glötzel, D. *Highlights of Condensed Matter Theory* Vol. LXXXIX 59 (Corso Soc. Italiana di Fisica, Bologna, 1985).
- Nørskov, J. K. *J. chem. Phys.* **90**, 7461–7471 (1989).
- Hammer, B. & Nørskov, J. K. *Surf. Sci.* (submitted).
- Payne, M. C., Teter, M. P., Allan, D. C., Arias, T. A. & Joannopoulos, J. D. *Rev. mod. Phys.* **64**, 1045–1097 (1992).
- Perdew, J. P. et al. *Phys. Rev.* **B46**, 6671–6687 (1992).
- Kittel, C. *Introduction to Solid State Physics* (Wiley, New York, 1968).

ACKNOWLEDGEMENTS. We thank B. I. Lundqvist, I. Chorkendorff, E. Törnqvist and A. Ruban for valuable input to this work. These calculations were performed on the JRCAT supercomputing system, which is supported by the New Energy and Industrial Technology Development Organization (NEDO) of Japan. The present work was in part supported by The Centre for Surface Reactivity which is sponsored by the Danish Research Councils; the Centre for Atomic-scale Materials Physics is sponsored by the Danish National Research Foundation.

Latitudinal gradient of atmospheric CO₂ due to seasonal exchange with land biota

A. Scott Denning*, Inez Y. Fung† & David Randall*

* Department of Atmospheric Science, Colorado State University, Fort Collins, Colorado 80521, USA

† National Aeronautics and Space Administration, Goddard Space Flight Center, Institute for Space Studies, 2880 Broadway, New York, New York 10025, USA and School of Earth and Ocean Sciences, University of Victoria, Victoria, British Columbia V8W 2Y2, Canada

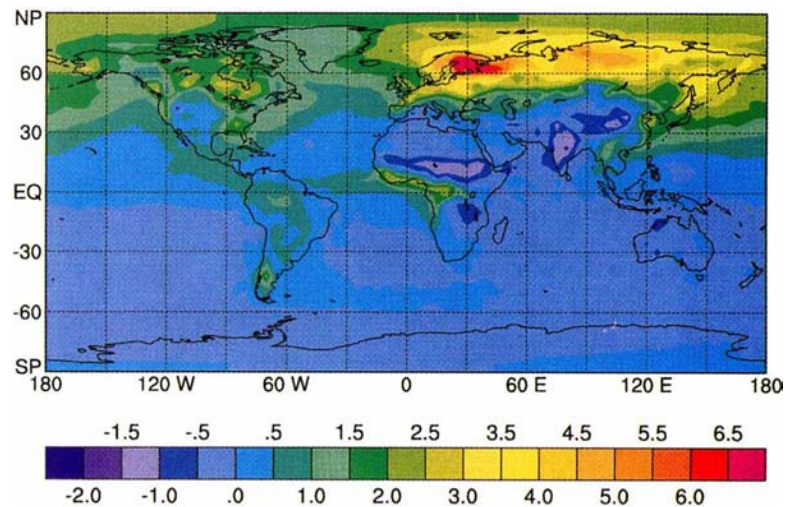
THE concentration of carbon dioxide in the atmosphere is increasing, largely because of fossil-fuel combustion, but the rate of increase is only about half of the total emission rate¹. The balance of the carbon must be taken up in the oceans and the terrestrial biosphere, but the relative importance of each of these sinks—as well as their geographical distribution and the uptake mechanisms involved—are still a matter of debate^{1–4}. Measurements of CO₂ concentrations at remote marine sites^{5–9} have been used with numerical models of atmospheric transport to deduce the location, nature and magnitude of these carbon sinks^{2,10–19}. One of the most important constraints on such estimates is the observed inter-hemispheric gradient in atmospheric CO₂ concentration. Published models that simulate the transport of trace gases suggest that the gradient is primarily due to interhemispheric differences in fossil-fuel emissions, with small contributions arising from natural exchange of CO₂ with the various carbon reservoirs. Here we use

a full atmospheric general circulation model with a more realistic representation of turbulent mixing near the ground to investigate CO₂ transport. We find that the latitudinal (meridional) gradient imposed by the seasonal terrestrial biota is nearly half as strong as that imposed by fossil-fuel emissions. Such a contribution implies that the sinks of atmospheric CO₂ in the Northern Hemisphere must be stronger than previously suggested.

Many previous studies of CO₂ transport in the atmosphere used the transport model developed at the Goddard Institute for Space Studies (GISS) of the National Aeronautics and Space Administration^{2,11–14,17,18}, which prescribes the three-dimensional wind field at four-hour time intervals from the output of an atmospheric general circulation model (GCM). Sub-grid-scale vertical transport of trace gases is simulated in terms of prescribed monthly mean convective frequencies in the parent GCM. Interhemispheric mixing in the model is tuned using an adjustable sub-grid diffusion parameter to produce realistic meridional gradients for tracers with known aseasonal, mid-latitude sources. The annual mean meridional gradient in atmospheric CO₂ simulated by the GISS model is much stronger than observed when the effects of fossil-fuel emissions, seasonal exchange with the terrestrial biota, and emissions from tropical deforestation and from the equatorial oceans are included (about 5 or 6 parts per million by volume (p.p.m.v.) from the Arctic to the Antarctic, as compared to an observed gradient of about 3 or 4 p.p.m.v.)². This implies the existence of sinks of CO₂ in the Northern Hemisphere so strong as to be inconsistent with available oceanographic data². Thus at least some of the Northern Hemisphere sink is believed to be terrestrial, and is thought to be due to direct CO₂ fertilization²⁰, nutrient deposition²¹, reforestation²² and/or climate fluctuations²³.

Although it has long been recognized that atmospheric dispersion of pollutants released at the ground surface depends

FIG. 1 Annual mean mixing ratio of CO₂ (colour scale; p.p.m.v.) in the planetary boundary layer (PBL) as simulated by the Colorado State University (CSU) GCM using surface fluxes representing the purely seasonal exchange with the terrestrial biosphere as calculated in ref. 14 and used in ref. 2. The value at the South Pole has been subtracted at every grid point. The concentration was initialized to be globally uniform, and the model was run on a coarse 7.2° × 9° grid with nine levels for a simulated ten years. The end of this "spin up" run was then used as the initial condition for a further four-year integration on a 4° × 5° grid with 17 levels. All results presented here are for the final three years of the 4° × 5° run. (NP, North Pole; EQ, Equator; SP, South Pole.)



strongly on the depth and intensity of near-surface atmospheric turbulence^{24,25}, this phenomenon has not been resolved in previous simulations of global CO₂ concentration. Because both atmospheric turbulence²⁵ and the surface flux of CO₂ (ref. 14) are strongly seasonal, correlations between these processes are likely to play an important role in determining the annual mean distribution of atmospheric CO₂. The GISS tracer model cannot represent such correlations adequately because only monthly mean statistics of convective mixing are employed, and the minimum mixing depth is that of the time-invariant lowest model layer.

We have repeated some of the calculations reported in ref. 2 using the Colorado State University (CSU) GCM^{26,28}, in which some important transport processes are represented more realistically than they can be in a tracer model. Surface fluxes of CO₂ were prescribed exactly as in ref. 2, but the tracer calculation was performed on-line in the GCM, at the model time step of six minutes. Penetrative vertical tracer transport by cumulus convection is calculated once per simulated hour. The lowest layer of the model atmosphere is represented as a well mixed planetary boundary layer (PBL), the depth of which is calculated prognostically in terms of the rates of turbulent entrainment and turbulence kinetic-energy dissipation, and loss of mass into cumulus clouds²⁹. Emissions of CO₂ from the surface are assumed to be immediately vertically mixed in this layer, and exert a greater effect on the PBL concentration under stable conditions when the PBL is shallow than under unstable conditions when the PBL is deep. A comparison of the seasonal variations of the simulated depth of the PBL and other near-surface meteorological variables in the GCM with the limited observational data available shows good agreement³⁰. The interhemispheric gradient of ⁸⁵Kr and vertical profiles of ²²²Rn simulated by the CSU GCM agree quite well with observations³¹ without the use of any tunable diffusion such as that used in the GISS model.

The seasonal drawdown of atmospheric CO₂ by photosynthesis and subsequent release of CO₂ by microbial respiration involve fluxes that are stronger than the anthropogenic emission rate by about an order of magnitude¹. These fluxes account for the very large seasonal amplitude of the annual cycle of CO₂ concentrations in the Northern Hemisphere^{1,10,19}. Although the prescribed seasonal CO₂ fluxes at the land surface are exactly balanced over an annual cycle¹⁴ (the net annual flux is zero at every grid point), they result in a non-uniform annual mean concentration field at the surface (Fig. 1). This effect has been noted by others, and has been attributed to the covariance of seasonal CO₂ exchange with meridional transport^{11,12} and with convective mixing^{12,18}. In the CSU GCM, the effect is enhanced

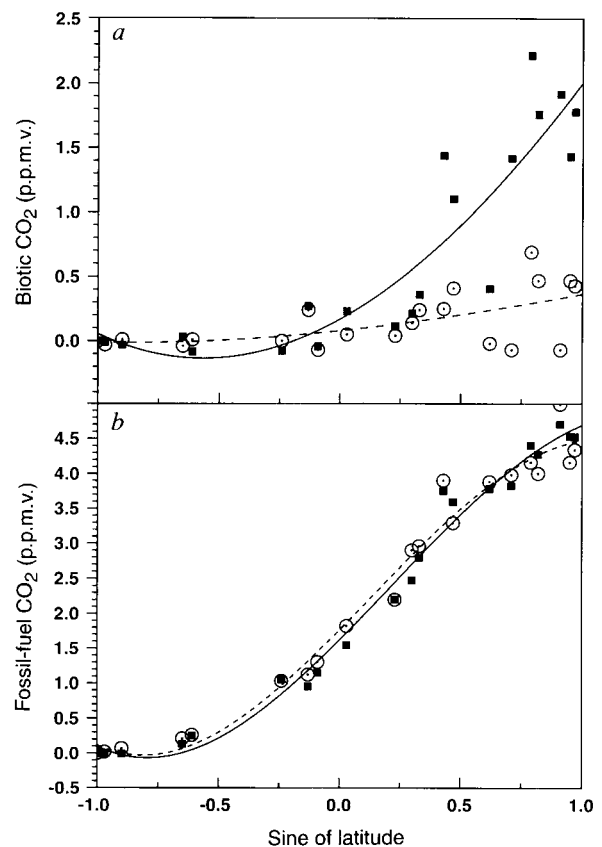


FIG. 2 Annual mean mixing ratio (p.p.m.v.) of simulated CO₂; a, using the seasonal biotic fluxes of ref. 2, and b, using the fossil-fuel emission estimates of ref. 2. Values are annual means in the PBL at the grid cells containing the 21 flask-sampling stations used in ref. 2. Where the grid cell was defined as land, we chose the adjacent cell offshore because flask-sampling protocol selects marine air only. Filled squares indicate values simulated by the CSU GCM, and open circles with a central dot indicate values simulated by the Goddard Institute for Space Studies (GISS) tracer model. The curves are cubic polynomials fitted by least-squares to the station values (the solid curves were fitted to the CSU GCM results, and the dashed curves were fitted to the GISS results). The value at the South Pole has been subtracted.

by the correlation between the seasonal CO_2 flux and vertical mixing by PBL turbulence. In regions with strongly seasonal vegetation, the CO_2 flux (to the atmosphere) is strongly negative at the peak of the summer growing season when both PBL turbulence and cumulus convection are active and vigorous, so air that has been depleted of CO_2 tends to be carried aloft. By contrast, in spring and autumn when CO_2 emissions from soil respiration exceed photosynthetic uptake, vertical mixing is weak or inactive, so the CO_2 -enriched air is confined to a thin layer close to the ground. This seasonal cycle gives rise to a net positive concentration anomaly in the annual mean.

At the remote marine locations sampled by the flask network⁹, the Arctic-to-Antarctic CO_2 gradient imposed by the purely seasonal fluxes at the land surface in the CSU GCM is more than four times as strong as the gradient simulated by the GISS tracer model (Fig. 2a). The difference in meridional gradients between the two models does not result from weaker meridional transport, as the simulated concentrations of fossil-fuel CO_2 at the locations of the flask stations are nearly identical (Fig. 2b). The simulated concentration fields arising from the fossil-fuel emissions and the seasonal vegetation are the subject of a tracer transport model intercomparison project (TRANSCOM), which is nearing completion (P. Rayner, personal communication). The meridional gradients simulated by the other models in the study vary considerably; the results presented here are within the range found by other participants in this project (unpublished results).

The difference between the simulated biogenic CO_2 concentrations in the two models is largest in the middle to high latitudes of the Northern Hemisphere (Fig. 2), where biotic CO_2 exchange with the atmosphere is most strongly seasonal¹⁴. Seasonal variations in biotic CO_2 flux and simulated vertical tracer transport by both cumulus convection and PBL turbulence are negatively correlated over this region (Fig. 3), and at the locations with the highest annual mean CO_2 concentrations, both of these cor-

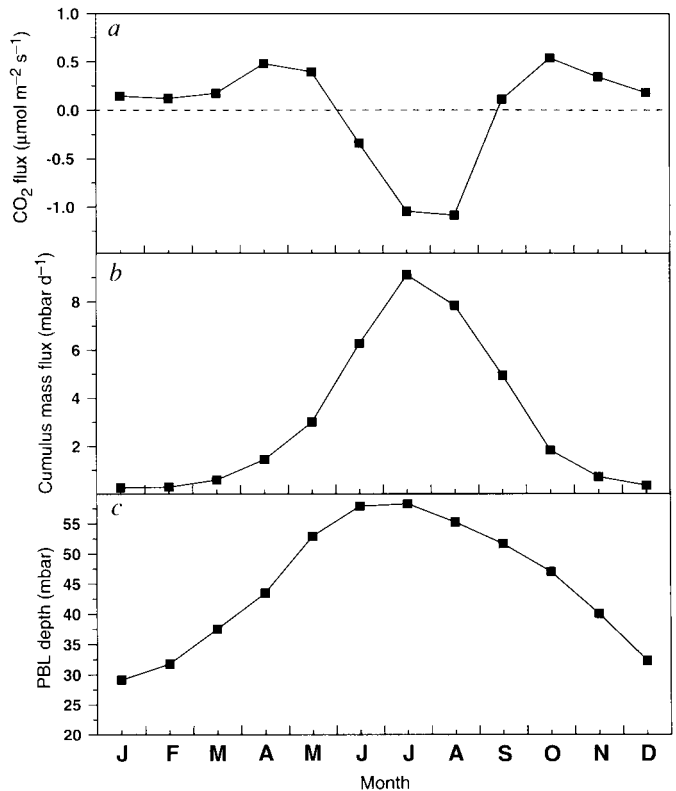


FIG. 3 Seasonal variations; a, of prescribed surface flux of CO_2 from the terrestrial biosphere to the atmosphere, b, of simulated atmospheric mass flux due to cumulus convection at the top of the atmospheric PBL, and c, of simulated depth of the atmospheric PBL. Values are area-weighted means for land points north of 28°N , averaged for each calendar month.

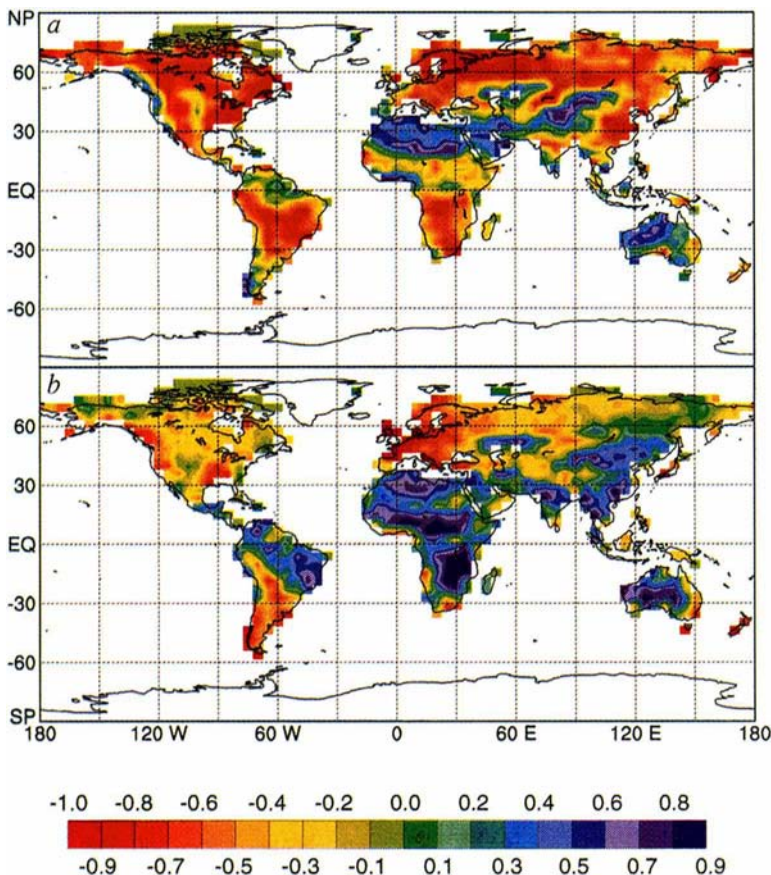


FIG. 4 Correlation coefficients (colour scale) of the relationship between prescribed monthly mean terrestrial surface CO_2 flux and; a, simulated cumulus mass flux at the top of the PBL, b, simulated depth of the PBL. The correlation was calculated separately at each land grid cell in the model, and the resulting values were contoured to produce the maps shown. Note that the colour scheme has been reversed (red indicates negative values and blue indicates positive values) for easier comparison with Fig. 1.

relations are very strong (Fig. 4). Over the tropics, where only cumulus convection is negatively correlated with CO₂ flux, the concentration is much lower. Because Fig. 4 presents the correlation rather than the covariance between the variables, the values vary independently of the magnitude of the CO₂ flux, and are therefore high in some regions (such as the Sahara) with little biological activity. These regions are characterized by minimal CO₂ concentration anomalies in the annual mean (Fig. 1). In view of the fact that PBL turbulence is not represented adequately in the GISS model, we conclude that the variable-depth PBL of the GCM has introduced a greater degree of correlation between the surface fluxes and vertical mixing over the temperate and boreal continents, and that this greater correlation has resulted in the higher annual mean CO₂ concentrations simulated for those regions.

Using the CSU GCM, the simulated meridional gradient in CO₂ concentration imposed by seasonal exchanges with the terrestrial biota (~2 p.p.m.v from pole to pole) is nearly half as strong as that imposed by the fossil-fuel emissions (~4.5 p.p.m.v.). This implies that the sinks of atmospheric CO₂ in the Northern Hemisphere must be even stronger than previously estimated². Calculation of the global carbon budget would require simulation of the effects of air-sea exchange, land use, and other sources and sinks, and is beyond the scope of this work, but the effect of the enhanced meridional gradient arising from the seasonal biotic fluxes would be significant. To illustrate the sensitivity of the calculated budget to the enhanced biogenic gradient, we substituted the CSU GCM results for the GISS results in the calculations of ref. 2. This leads to an 'extra' 1.5 p.p.m.v of CO₂ at high northern latitudes that is not observed and must be offset without violating the observed annual mass balance of the atmosphere. The excess CO₂ could be offset by an additional Northern Hemisphere sink of 1.2–2.5 Gt C yr⁻¹ (depending on the proximity of the sink to the flask stations) relative to ref. 2. Such a sink would have to be compensated by an equatorial source of the same magnitude, yielding a deforestation rate of 2–3.5 Gt C yr⁻¹, which exceeds current estimates for this source¹. Alternatively, the stronger meridional gradient in CO₂ concentration simulated by the CSU GCM could be compensated by an extra sink of 0.6 Gt C yr⁻¹ in the Northern Hemisphere, and a Southern Hemisphere sink that is weaker by the same amount. This would yield a sink strength of only 1.0–1.2 Gt C yr⁻¹ for the ocean gyres in the Southern Hemisphere². □

Received 4 January; accepted 23 June 1995.

- Schimmel, D. et al. in *Climate Change 1994: Radiative Forcing of Climate Change and An Evaluation of the IPCC IS92 Emission Scenarios* (eds Houghton, J. T. et al.) 39–71 (Cambridge Univ. Press, 1994).
- Tans, P. P., Fung, I. Y. & Takahashi, T. *Science* **247**, 1431–1438 (1990).
- Sarmiento, J. L., Orr, J. C. & Siegenthaler, U. *J. geophys. Res.* **97**, 3621–3645 (1992).
- Sarmiento, J. L. & Sundquist, E. T. *Nature* **356**, 589–593 (1992).
- Fraser, P. J., Pearman, G. I. & Hyson, P. J. *geophys. Res.* **88**, 3591–3598 (1983).
- Conway, T. J. et al. *Tellus* **40B**, 81–115 (1988).
- Keeling, C. D. & Whorf, T. P. in *Trends '93: A Compendium of Data on Global Change* (eds Boden, T. A., Kaiser, D. P., Sepanski, R. J. & Stoss, F. W.) 16–27 (ORNL/CDIAC-65, Carbon Dioxide Information Analysis Center, Oak Ridge National Laboratory, Oak Ridge, TN, 1994).
- Trivett, N. B. A., Hudec, V. C. & Wong, C. S. in *Trends '93: A Compendium of Data on Global Change* (eds Boden, T. A., Kaiser, D. P., Sepanski, R. J. & Stoss, F. W.) 120–130 (ORNL/CDIAC-65, Carbon Dioxide Information Analysis Center, Oak Ridge National Laboratory, Oak Ridge, TN, 1994).
- Conway, T. J. et al. *J. geophys. Res.* **99**, 22831–22855 (1994).
- Pearman, G. I., Hyson, P. J. & Fraser, P. J. *J. geophys. Res.* **88**, 3581–3590 (1983).
- Fung, I., Prentice, K., Matthews, E., Lerner, J. & Russell, G. *J. geophys. Res.* **88**, 1281–1294 (1983).
- Heimann, M., Keeling, C. D. & Fung, I. Y. in *The Changing Carbon Cycle: A Global Analysis* (eds Trabalka, J. R. & Reichle, D. E.) 16–49 (Springer, New York, 1986).
- Fung, I. Y. in *The Changing Carbon Cycle: A Global Analysis* (eds Trabalka, J. R. & Reichle, D. E.) 459–473 (Springer, New York, 1986).
- Fung, I. Y., Tucker, C. J. & Prentice, K. C. *J. geophys. Res.* **92**, 2999–3015 (1987).
- Tans, P. P., Conway, T. J. & Nakazawa, T. *J. geophys. Res.* **94**, 5151–5172 (1989).
- Enting, I. G. & Mansbridge, J. V. *Tellus* **39B**, 318–325 (1989).
- Heimann, M. & Keeling, C. D. in *Aspects of Climate Variability in the Pacific and Western Americas* (ed. Peterson, D. H.) 237–275 (Geophys. Monogr. 55, Am. Geophys. Union, Washington DC, 1989).
- Keeling, C. D., Piper, S. C. & Heimann, M. in *Aspects of Climate Variability in the Pacific and Western Americas* (ed. Peterson, D. H.) 305–363 (Geophys. Monogr. 55, Am. Geophys. Union, Washington DC, 1989).
- Enting, I. G. & Mansbridge, J. V. *Tellus* **43B**, 156–170 (1991).
- Gifford, R. M. *Aust. J. Pl. Physiol.* **21**, 1–15 (1994).
- Schindler, D. W. & Bayley, S. E. *Global Biogeochem. Cycles* **7**, 717–734 (1993).

- Dixon, R. K. et al. *Science* **263**, 185–190 (1994).
- Dal, A. & Fung, I. Y. *Global Biogeochem. Cycles* **7**, 599–610 (1993).
- Pasquill, F. *Met. Mag.* **90**, 33–49 (1961).
- Stull, R. B. *An Introduction to Boundary Layer Meteorology* (Kluwer Academic, Dordrecht, 1988).
- Randall, D. A., Harshvardhan, Dazlich, D. A. & Corsetti, T. G. *J. Atmos. Sci.* **46**, 1943–1970 (1989).
- Randall, D. A., Harshvardhan & Dazlich, D. A. *J. Atmos. Sci.* **48**, 40–62 (1991).
- Randall, D. A. & Pan, D.-M. in *The Representation of Cumulus Convection in Numerical Models* (eds Emanuel, K. & Raymond, D.) 137–144 (Met. Monogr. 24, Am. Meteorological Soc., Boston, 1993).
- Suarez, M., Arakawa, A. & Randall, D. A. *Mon. Weath. Rev.* **111**, 2224–2243 (1983).
- Randall, D. A., Abeles, J. A. & Corsetti, T. G. *J. Atmos. Sci.* **42**, 641–676 (1985).
- Denning, A. S. *Investigations of the Transport, Sources, and Sinks of Atmospheric CO₂ Using a General Circulation Model* (Atmos. Sci. Pap. 564, Colorado State Univ., Fort Collins, CO, 1994).

ACKNOWLEDGEMENTS. This work was supported by the US National Aeronautics and Space Administration (NASA) under the Global Change Fellowship Program and the Earth Observing System—Interdisciplinary Science. I.Y.F. was also supported by the Carbon Dioxide Research Program of the US Department of Energy. Computing support was provided by the NASA Center for Computational Sciences.

Atmospheric inputs of dissolved organic nitrogen to the oceans

S. Cornell, A. Rendell* & T. Jickells

School of Environmental Sciences, University of East Anglia, Norwich NR4 7TJ, UK

THE input of fixed nitrogen to the oceans by *in situ* fixation, river/groundwater supply and atmospheric deposition represents an important control on marine productivity on long timescales, and hence on ocean-atmosphere CO₂ exchange and its effects on climate^{1–3}. Any assessment of human perturbation of the global nitrogen cycle also requires an accurate estimate of these inputs. The current best estimates suggest that the natural fluvial and atmospheric inputs are of similar magnitude^{3,4}, and that globally both have been increased by a factor of two above natural levels as a result of human activity^{3–5}. Dissolved organic nitrogen represents more than half of the fluvial input of dissolved fixed nitrogen, but current estimates of atmospheric inputs are usually based on only the inorganic (NO₃⁻ + NH₄⁺) component, although some authors have recognized the potential importance of organic nitrogen^{6–9}. Here we present analyses of dissolved organic nitrogen in rain and snow which show that it is a ubiquitous and significant component of precipitation, even in remote marine areas. Our results require an approximate doubling of present estimates of the atmospheric input of fixed nitrogen to the oceans, and an increase in estimates of the total fixed-nitrogen input by a factor of about 1.5. These results indicate that the human impact on the global nitrogen cycle may be larger than has been thought.

Rainwater samples from various locations have been collected and analysed for nitrate, ammonium and dissolved organic nitrogen (DON) (Table 1). The first and clearest conclusion of this study is that, although average concentrations vary considerably between locations, DON is a ubiquitous component of rain water, and in remote marine locations it is the dominant form of fixed nitrogen. Atmospheric fixed-nitrogen budgets must clearly include DON. This conclusion raises the question of the origin—whether marine or terrestrial—and the composition of this DON.

The chemical composition of atmospheric, and marine, organic matter is largely unknown^{10,11}. At continental sites, atmospheric DON seems to be a biologically available nitrogen source with urea an important constituent¹². Other studies report half the reduced nitrogen in aerosols to be organic and relatively

* Present address: School of Biological and Molecular Sciences, Oxford Brookes University, Oxford OX3 0BP, UK.